Journal Pre-proof

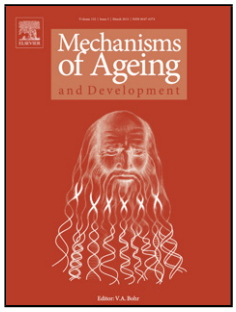

ATM-deficient neural precursors develop senescence phenotype with disturbances in autophagy

Piotr Sunderland, Justyna Augustyniak, Jacek Lenart, Leonora Bużańska, Luigi Carlessi, Domenico Delia, Ewa Sikora

PII: S0047-6374(20)30092-0

DOI: https://doi.org/10.1016/j.mad.2020.111296

Reference: MAD 111296

To appear in: *Mechanisms of Ageing and Development*

Received Date: 22 November 2019

Revised Date: 29 May 2020

Accepted Date: 22 June 2020

Please cite this article as: Sunderland P, Augustyniak J, Lenart J, Bużańska L, Carlessi L, Delia D, Sikora E, ATM-deficient neural precursors develop senescence phenotype with disturbances in autophagy, *Mechanisms of Ageing and Development* (2020), doi: https://doi.org/10.1016/j.mad.2020.111296

ATM-DEFICIENT NEURAL PRECURSORS DEVELOP SENESCENCE PHENOTYPE WITH DISTURBANCES IN AUTOPHAGY

Piotr Sunderland[1*], Justyna Augustyniak[2], Jacek Lenart[2], Leonora Bużańska[2], Luigi Carlessi[3], Domenico Delia[3,4], Ewa Sikora[1*]

[1]Nencki Institute of Experimental Biology, Polish Academy of Sciences, Warsaw, Poland,
[2]Mossakowski Medical Research Centre, Polish Academy of Sciences, Warsaw, Poland,
[3]Department of Research, Fondazione IRCCS Istituto Nazionale Tumori, Milan, Italy
[4]IFOM, FIRC Institute of Molecular Oncology, Milano, Italy

*Corresponding authors:
Piotr Sunderland
Nencki Institute of Experimental Biology, Polish Academy of Sciences,
3 Pasteura St.
02-093 Warsaw, Poland
email: p.sunderland@nencki.edu.pl

Prof. Ewa Sikora
Nencki Institute of Experimental Biology, Polish Academy of Sciences,
3 Pasteura St.
02-093 Warsaw, Poland
email: e.sikora@nencki.edu.pl

Highlights

- ATM-deficient neural progenitors display markers of senescence and oxidative stress
- general autophagy and mitophagy are impaired in ATM-deficient neural progenitors
- external sources of oxidative stress partially aggravate the observed phenotype
- ataxia-telangiectasia disease may have a component of neuronal senescence

ABSTRACT

ATM is a kinase involved in DNA damage response (DDR), regulation of response to oxidative stress, autophagy and mitophagy. Mutations in the ATM gene in humans result in

ataxia-telangiectasia disease (A-T) characterized by a variety of symptoms with neurodegeneration and premature ageing among them. Since brain is one of the most affected organs in A-T, we have focused on senescence of neural progenitor cells (NPCs) derived from A-T reprogrammed fibroblasts. Accordingly, A-T NPCs obtained through neural differentiation of iPSCs in 5% oxygen possessed some features of senescence including increased activity of SA-β-gal and secretion of IL6 and IL8 in comparison to control NPCs. This phenotype of A-T NPC was accompanied by elevated oxidative stress. A-T NPCs exhibited symptoms of impaired autophagy and mitophagy with lack of response to chloroquine treatment. Additional sources of oxidative stress like increased oxygen concentration (20%) and H_2O_2 respectively aggravated the phenotype of senescence and additionally disturbed the process of mitophagy. In both cases only A-T NPCs reacted to the treatment. We conclude that oxidative stress may be responsible for the phenotype of senescence and impairment of autophagy in A-T NPCs. Our results point to senescent A-T cells as a potential therapeutic target in this disease.

Keywords: ATM, ataxia-telangiectasia, autophagy, hiPSCs, mitophagy, neural progenitors, senescence, oxidative stress

Abbreviations

4HNE – 4-hydroxynonenal; ***ACTB* –** Actin Beta; **A-T –** ataxia-telangiectasia; **ATM –** ataxia-telangiectasia mutated; ***BNIP3*** – Homo sapiens BCL2 interacting protein 3; ***CAPN10*** – Calpain 10, Calcium-Activated Neutral Proteinase 10; ***CCNG1*** – Cyclin G1; **CQ** – chloroquine; **DDR** – DNA damage response; **DHE** – dihydroethidium; **DSBs** –double strand breaks; ***EEF1A1*** – Eukaryotic Translation Elongation Factor 1 Alpha 1; ***EID2*** – EP300 Interacting Inhibitor Of Differentiation 2; ***FUNDC1*** – Homo sapiens FUN14 domain containing 1; ***GAPDH*** – Glyceraldehyde-3-Phosphate Dehydrogenase; ***GFAP*** – Homo sapiens glial fibrillary acidic protein; ***HPRT1*** – Hypoxanthine Phosphoribosyltransferase 1; **IL6** – interleukin 6; **IL8** – interleukin 8; **IPSCs** – Induced pluripotent stem cells; **LAMP2** – lysosome-associated membrane protein 2; **LC3** – microtubule-associated protein 1B light chain 3; ***MAP2*** – Homo sapiens microtubule associated protein 2; **MAPK** – mitogen-activated protein kinase; ***MT-ATP6*** – Mitochondrially Encoded ATP Synthase Membrane Subunit 6; ***MYC*** – V-Myc Avian Myelocytomatosis Viral Oncogene Homolog; **NOX4** – NADPH oxidase 4; **NPC** – neural progenitor cells; ***OGG1*** – Homo sapiens 8-oxoguanine DNA glycosylase; ***PHB*** – Prohibitin; ***PARK2 (PARKIN)*** – Homo sapiens parkin RBR E3

ubiquitin protein ligase (PRKN); **PSD95** – postsynaptic density protein 95***RABEP2*** – Rabaptin, RAB GTPase Binding Effector Protein 2; **ROS** – reactive oxygen species; ***RPLP0*** – Ribosomal Protein Lateral Stalk Subunit P0; **SA-β-Gal** – senescence-associated β-galactosidase; **SASP** – senescence-associated secretory phenotype; ***SCLO2B1*** – solute carrier organic anion transporter family, member 2B1; **SIRT1** – Homo sapiens sirtuin 1; ***SOD1*** – Homo sapiens superoxide dismutase 1; ***TBP*** – TATA-Box Binding Protein; **TOM20** – translocase of the outer mitochondrial membrane; ***TUBB3*** – beta Tubulin class III (BTUB); ***UBC*** – Ubiquitin C; ***VAMP2*** – Homo sapiens vesicle associated membrane protein 2; ***ZNF324B*** – Zinc Finger Protein 324B

INTRODUCTION

ATM (Ataxia Telangiectasia Mutated) is a serine/threonine kinase belonging to the superfamily of phosphatidylinositol 3-kinase-related kinases. It plays a crucial role in DNA damage response pathway (DDR) where it is activated by DNA double-strand breaks (DSBs). Upon phosphorylation, ATM activates several proteins belonging to DDR, leading in turn to cell cycle arrest, cell senescence, DNA repair or apoptosis. In addition to this, growing evidence suggests that ATM is a regulator of oxidative stress response, mitochondrial homeostasis and autophagy [Stagni et al., 2018].

Mutations in the ATM gene result in ataxia-telangiectasia (A-T), a rare recessive human disease, characterized by radiosensitivity, susceptibility to cancer, immunodeficiency, telangiectasia, premature ageing and neurodegeneration with progressive cerebellar atrophy [Shiloh et al., 2013]. Patients develop a variety of neurological symptoms beginning with balancing problems in early childhood and leading to slurred speech severe ataxia later in life. Lifespan of A-T patients varies, but generally does not exceed early thirties.

While radiosensitivity and higher cancer incidents can be easily explained by defective DNA damage response and repair, the basis of neurodegeneration in A-T is not fully resolved. Dysregulated cell cycle control leading to cycle re-entry [Yang et al., 2005], synaptic dysfunction [Li et al., 2009] and mitochondrial abnormalities [Choy and Watters 2018] are among the hypotheses. In addition to this, emerging role of ATM in response to cellular ROS brings more attention to oxidative stress in A-T. Fibroblasts and lymphocytes from A-T patients exhibit higher levels of reactive oxygen species (ROS), so do tissues of A-T mouse models [Kamsler et al., 2001, Lee et al., 2001]. Increased sensitivity to ROS-generating agents in patients-derived fibroblasts has also been reported [Ward et al., 1994].

These findings led to description of alternative pathway of ATM activation which is DNA-damage independent. In 2010 Guo et al., [Guo et al., 2010] identified this non-canonical activation of ATM in the absence of DSBs. The oxidized, self-activated ATM turns into a disulfide-cross-linked dimer working as a sensor of oxidation. This form triggers further response to oxidative stress affecting, among others, glutathione synthesis and pentose phosphate pathway [Cosentino et al., 2011].

One of downstream effects of activating ATM upon oxidative stress is maintenance of proteostasis via autophagy. Autophagy (the term commonly used for macroautophagy) is a tightly regulated, complex and very dynamic process resulting in digestion of cell organelles and various aggregates. ATM activates autophagy by inhibiting its negative regulator – mTOR, enabling in turn proper formation of autophagic vesicles. This way, in the presence of activated ATM, autophagy proceeds further to the fusion of autophagosome with lysosome and digestion of cargo [Alexander et al., 2010]. Also mitophagy, the process of selective removal of damaged mitochondria, has been shown to be partially dependent on ATM. This mechanism requires further investigation, but so far there is strong evidence, that loss of ATM causes accumulation of dysfunctional mitochondria with ROS overproduction [Stagni et al., 2018].

A-T patients suffer from a variety diseases and symptoms commonly identified as age-related conditions (diabetes, liver fibrosis, premature greying of hair), some of which have been previously associated with accumulation of senescent cells [Barzilai et al., 2017]. Despite that apparent link, cell senescence has not been studied much in these individuals. The state of cellular senescence is generally defined as a permanent proliferation arrest in which cells remain metabolically active. It is distinguished from other cells fates where proliferation arrest occurs by a consistent phenotype characterized by altered morphology, increased activity of senescence-associated β-galactosidase (SA-β-gal) – widely used as a marker of senescence [Dimri et al., 1995] – and other features such as senescence-associated secretory phenotype (SASP), persistent DNA damage, modifications of chromatin and the presence of cell cycle inhibitors, e.g. p16 and p21 [van Deursen 2014, López-Otin et al., 2013]. Accumulation of senescent cells during ageing is already a well-established fact [Campisi 2011], so is their role in some age-related pathologies [van Deursen 2014]. Moreover, genetic or pharmacological reduction of senescent cell burden is associated with delay, prevention, or alleviation of multiple age-related conditions [Kirkland and Tchkonia 2017, Sikora et al., 2019].

Until recently, the term cellular senescence has been used only for proliferation-competent cells. However, a considerable amount of recent literature suggests that even non-dividing, differentiated cells may be characterized as senescent under certain circumstances [Sapieha and Mallette 2018, Anderson et al, 2019]. Since majority of cells in mammalian organisms are post-mitotic, this area of study may be crucial for explaining some age-related changes.

In the case of neurons, markers such as SA-β-gal, phosphorylation of p38 kinase, activation of DNA damage response (DDR) and proinflammatory cytokines, were found in neurons of 32-month old but not of 4-month-old mice [Jurk et al., 2012]. Other recent studies, including ours, show an increase in the number of neurons with active SA-β-gal in the hippocampi of old mice in comparison with young animals' neurons [Piechota et al., 2016, Geng et al., 2010]. Increased number of these cells was also documented in our study in a long term culture of cortical neurons; interestingly this increase seemed not to be caused by DNA damage or DDR activation [Piechota et al., 2016].

The role of autophagy in establishing cell senescence is not obvious and has been recently a matter of scientific debate [Kang et al., 2016]. While it is agreed that autophagy is a cytoprotective process, experimental data show it to be both positively and negatively linked to cellular senescence, proving it to be dependent on the cellular context [Gewirtz 2013]. Yet, it is mostly the disturbance in proteostasis that is associated with ageing, including ageing of the brain [Lipinski et al., 2010]. Recently, selective autophagy of GATA4 transcription factor has been shown to be crucial for establishing cell senescence phenotype, including SASP [Kang et al., 2015].

Given that A-T patients demonstrate numerous signs of accelerated ageing it could be expected that cells derived from A-T patients are more susceptible to cellular senescence. Indeed, signs of premature senescence have been shown in AT-derived fibroblasts [Shiloh et al., 1982, Polubotko et al., 2009]. No previous study, however, dealt with cellular senescence in A-T neurons, even though brain is the organ that shows so many symptoms of the disease. Here, by using non-dividing late neural progenitor cells (NPCs) as an approximation of human neurons, we aim to examine whether NPCs derived from A-T patients develop a senescence phenotype *in vitro* and elucidating the underlying molecular mechanisms. This paper also attempts to shed some light on the process of senescence in differentiated cells obtained from hiPSCs and in non-dividing cells in general. Moreover, we attempt to link senescence of non-dividing cells with autophagy and oxidative stress.

RESULTS

Characterization of hiPSCs-derived NPCs

Early NPCs were obtained from an A-T patient and a healthy individual through reprogramming of fibroblasts to hiPSCs and their further neural differentiation as described in details in [Carlessi et al., 2014] and as detailed in the "Materials and methods" section.

As the area of interest of this study were non-dividing brain cells, early NPCs were further differentiated into late NPCs by removal of two growth factors (EGF and FGF) from culture medium. After 14 days, NPCs changed their morphology (Fig. 1A) and had a well-developed web of dendrites as marked by MAP2 (Fig. 1B) and β-tubulin type III staining (Fig. 1C). Representative image of the culture from this stage (Fig. 1B) shows that only single cells were still proliferating (Ki67 staining). No differences in this regard were observed between A-T and control NPCs. Western blot of postsynaptic density protein (PSD95) provides evidence that synapses at this stage were already forming (Fig. 1D, upper panel). We also demonstrated that the A-T genotype was preserved throughout the reprogramming process (Fig.1D, lower panel). Cells at all stages were kept in 5% oxygen concentration (if not shown otherwise), considered to be conditions of physiological normoxia.

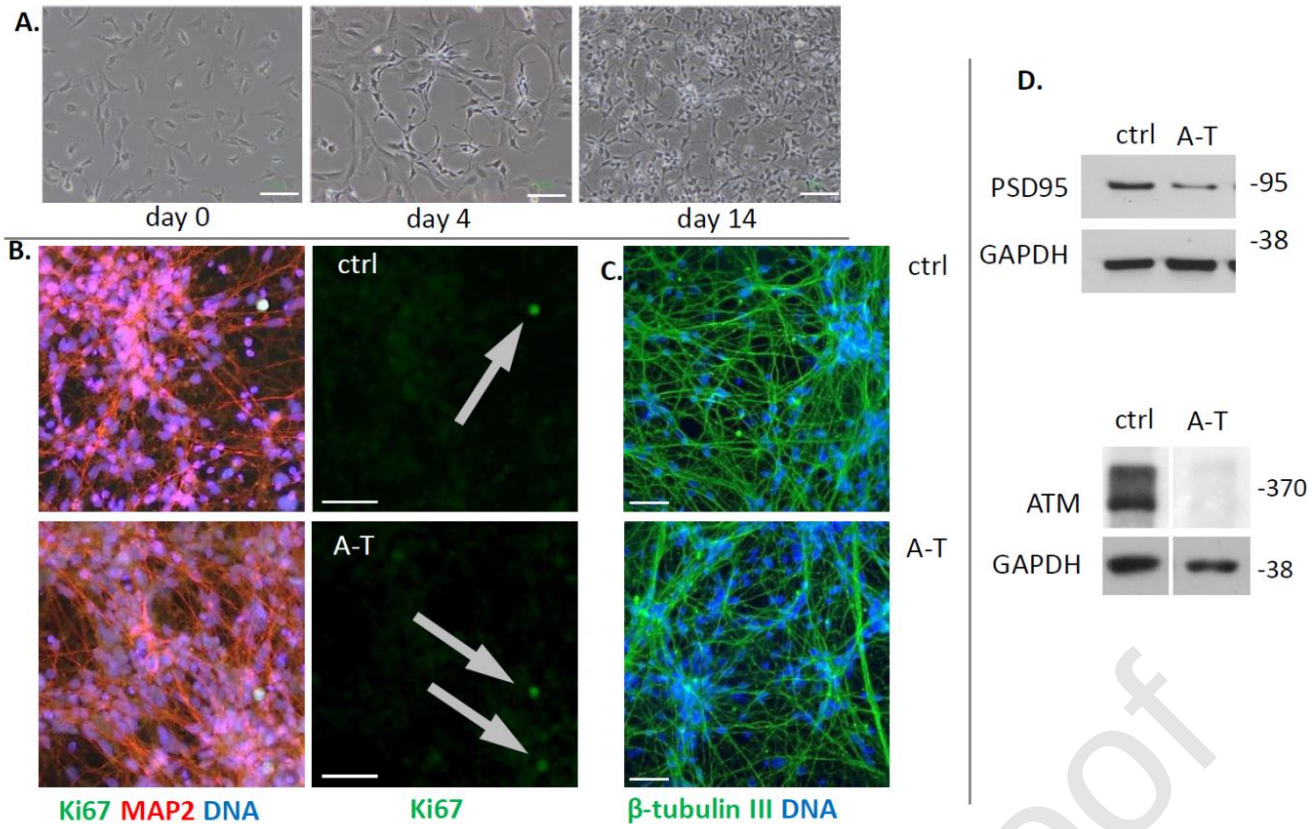

Figure 1. Characterization of hiPSCs-derived NPCs. A. Representative brightfield images of NPCs differentiated for 14 days. All of the subsequent images represent NPCs after 14 days of differentiation. Scale bars represent 50 µm. B. Representative images of Ki67 (green) and MAP2 (red) staining in A-T and control NPCs. Positive nuclei indicated by arrows. Scale bars represent 50 µm. C. Representative images of β-tubulin type III (green) immunostaining in A-T and control NPCs. Scale bars represent 50 µm. D. Representative immunoblots showing the level of PSD95 and ATM proteins in A-T and control NPCs (n=3).

A-T NPCs exhibit markers of cell senescence

In order to compare the number of senescent cells among A-T and control NPCs, several well-established markers of senescence were assessed. SA-β-gal, a classic hallmark of senescence, was examined in a 14-day culture described above. Additional staining of MAP2 was included after SA-β-gal test to make sure that only MAP2-positive cells were allowed in the final count. Figure 2A demonstrates that there was a significantly higher number of cells with active SA-β-gal in the population of A-T NPCs.

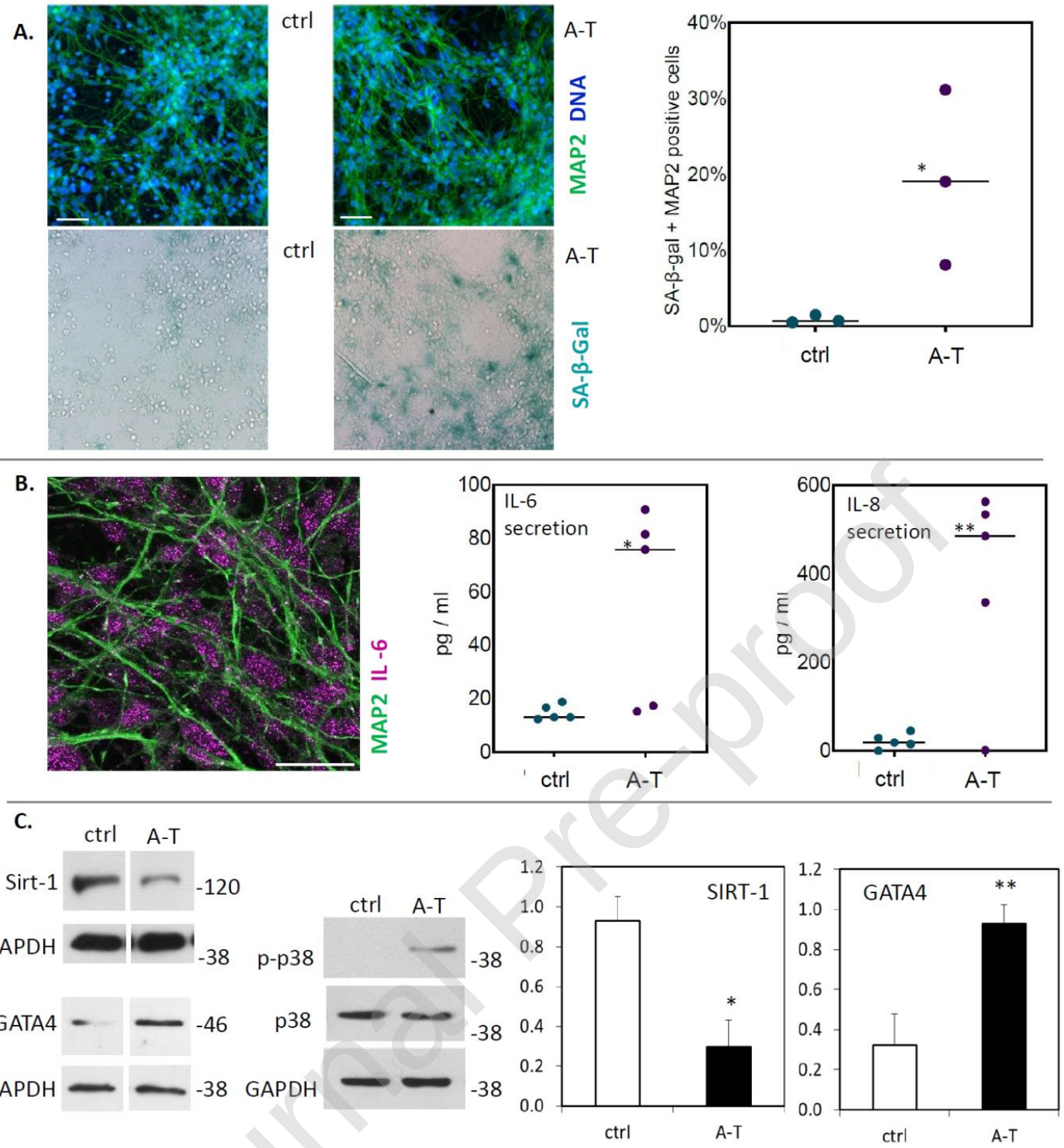

Figure 2. ATM-deficient NPCs exhibit senescence-like features. A. Representative images of SA-β-gal (blue) staining in control and A-T NPCs after 14-day differentiation (bottom images). Cells have been additionally stained for MAP2 in green and DNA in blue (top images). Top and bottom pictures represent the same areas. Scale bars represent 50 µm. Quantification of SA-β-gal staining. NPCs positive for both MAP2 and SA-β-gal were counted and divided by the total number of cells, as estimated by the number of nuclei (n=3). B. Senescence associated inflammatory cytokines. Representative confocal microscopy images of Interleukin 6 (magenta) and MAP2 (green) showing production of IL-6 in A-T NPCs. Scale bar represents 25 µm. ELISA test for IL-6 and IL-8 showing the level of secretion to medium (n=5). C. Immunoblots of SIRT1, GATA4 and p-p38 protein levels from control and A-T NPCs (n=3). Bars represent mean values of band intensity with SD after normalizing to GAPDH level.

SASP consists of inflammatory cytokines (with a predominance of IL-6), growth factors, and proteases varying in composition between different cell types and stimuli. It is considered as one of the crucial features of cell senescence [Rodier et al., 2009]. Cytokines

released by one cell may influence the environment and induce non-autonomous cell senescence [Kuilman et al., 2010]. Here we employed ELISA test to measure cytokine quantities released to the medium. Our results showed that the level of IL-6 was on average four times higher in A-T NPCs and even up to thirty times higher in the case of secretion of IL-8 (Fig. 2B), however, these amounts strongly varied between cultures and in some repetitions they were similar in two groups. Immunostaining for IL- 6 shows production of this cytokine in MAP2-positive NPCs (Fig.2B).

SIRT1 is a NAD-dependent deacetylase belonging to the SIRT protein family considered as "proteins of youth" [Grabowska et al., 2017]. In our experimental setup we have found that the level of SIRT1 was about three times lower in A-T NPCs, pointing again to their senescence (Fig. 2C).

We further looked at GATA4 transcription factor – a positive regulator of SASP found in multiple ageing tissues, including brain. According to Kang et al., [Kang et al., 2015], GATA4 positively regulates secretion of proinflammatory cytokines via NFκB. Western blot analysis revealed increased level of the GATA4 protein in A-T NPCs confirming their senescence (Fig. 2D). Also, the level of p38 MAPK, another factor involved in regulation of proinflammatory cytokines in a DNA damage-independent manner [Freund et al., 2011], was higher in A-T NPCs (Fig.2D). Collectively, we show that A-T NPCs, cultivated in physiological normoxia (5%), displayed some characteristics of cell senescence, which were not observed in control NPCs.

Senescent phenotype in A-T NPCs may be oxidative stress-dependent

A number of previous studies reported elevated oxidative stress in cells derived from A-T patients [Barlow et al., 1999, Kamsler et al., 2001]. This phenomenon has its roots in the lack of protection provided by ATM, which, as mentioned before, works as a sensor of oxidative stress. Another contributing factor correlating with ATM-deficiency is an elevated level of NOX-4. It has been reported that the level of this ROS-producing enzyme is raised in cerebral cortex of A-T patients and ATM knock-out [Weyemi et al., 2015]. Here we show that A-T NPCs also have approximately 4-times more NOX-4 than control NPCs (Fig. 3A).

These two factors, namely the lack of ATM and increased level of NOX-4, result in increased oxidative stress in A-T cells. As can be seen in Figure 3B, we have detected higher levels of 4-HNE, a "footprint" of oxidation, compared to control NPCs. It is a stable product of lipid peroxidation that binds nonspecifically to proteins and can be therefore detected in western blot analysis (Fig.3B).

In addition to this, we observed impaired antioxidant defense in A-T NPCs. Namely, the expression of *SOD1*, a gene coding Cu/Zn superoxide dismutase, a major antioxidant enzyme that catalyzes the conversion of superoxide anion to hydrogen peroxide and molecular oxygen [Fridovich et al., 1989], was significantly reduced in A-T NPCs in comparison to control NPCs (Fig. 3B).

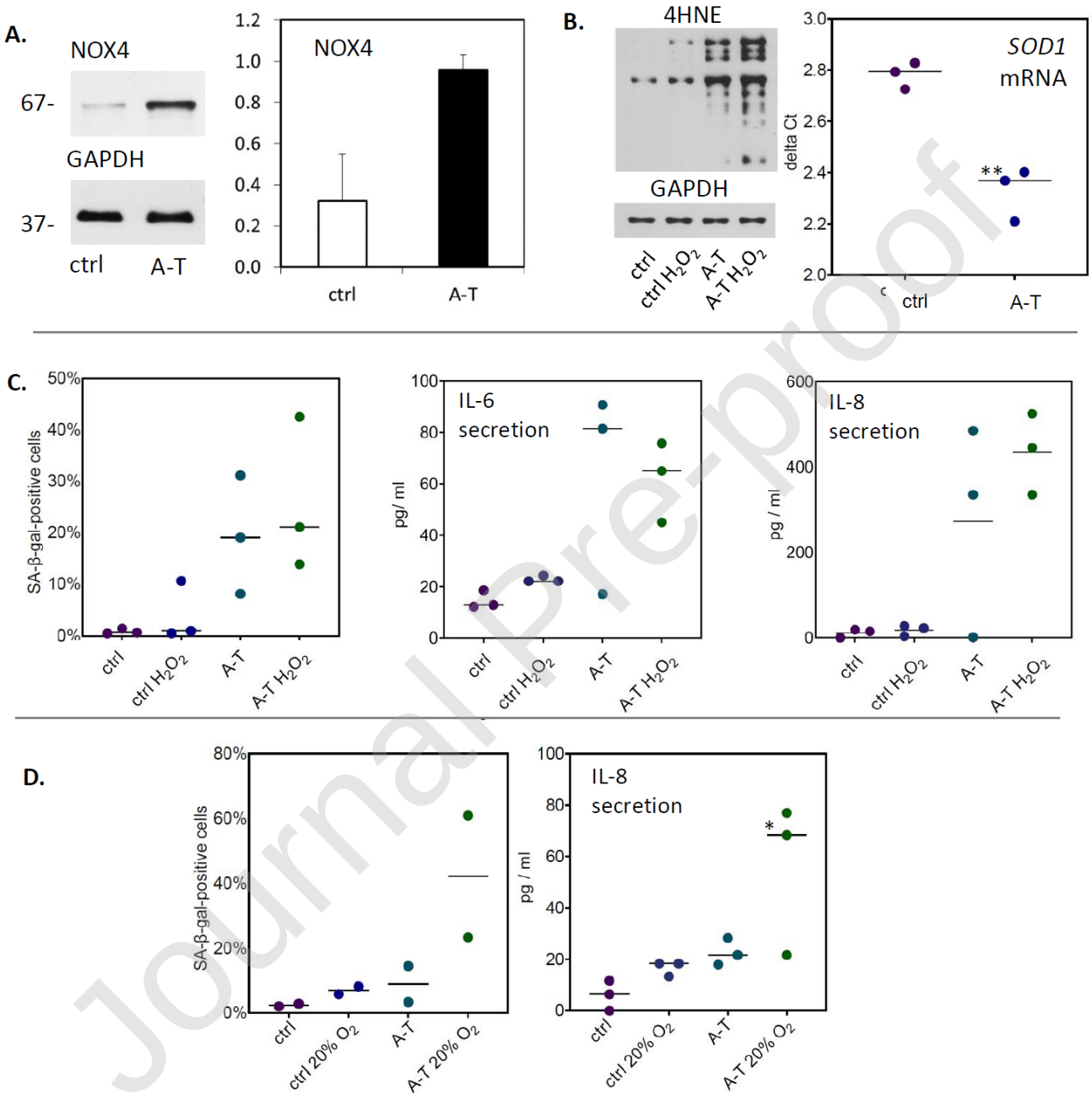

Figure 3. Senescent-like phenotype in ATM-deficient NPCs is partially oxidative-stress dependent. A. Immunoblot of NOX4 protein from control and A-T neural NPCs (n=3). Bars represent mean values of band intensity with SD. B. Immunoblot of 4-HNE protein modification (n=3). Expression level of *SOD1* (n=3). *C.* Quantification of SA-β-gal staining and IL-6 and IL-8 secretion in cells treated with hydrogen peroxide (n=3). D. Quantification of SA-β-gal staining (n=2) and IL-8 secretion under normoxic (5% oxygen) and hyperoxic (20% oxygen) conditions (n=3).

From this point, we decided to investigate whether oxidative stress may be the factor underlying the observed features of cellular senescence in A-T NPCs. Two sources of external oxidative stress have been used to potentially aggravate this phenotype. We treated the NPCs with 15 μM H_2O_2 and collected the cells after 4 days. Average number of NPCs with active SA-β-gal remained statistically unchanged, however, an upward trend was observed (Fig. 3C). We did not observe increased IL-6 and IL-8 secretion in A-T NPCs cells upon H_2O_2 treatment.

To intensify the exposure to oxidative stress, another approach was employed. To impose chronic hyperoxic conditions, plates with NPCs (A-T and control) were moved to a standard incubator with 20% oxygen, where they were left to differentiate into non-dividing NPCs. Cells kept in 5% oxygen served as non-treated control. As shown in Figure 3D, atmospheric conditions had a significant effect in this model. The percentage of A-T NPCs with increased activity of SA-β-gal rose to about 40% compared to those kept in 5% oxygen. Control NPCs did not show any change in SA-β-gal activity which indicates a protective role of the ATM protein in these cells. Furthermore, we collected media from cells cultivated in both conditions and compared the level of IL-8. It appeared that in 20% oxygen IL-8 secretion was three times higher in A-T cells compared with those kept in 5% (Fig. 3D). No changes in IL-6 secretion were detected.

Altogether, we showed that A-T NPCs appeared to be less protected (lack of ATM and decreased expression of *SOD1*) against internal (NOX-4) and external (20% of oxygen) oxidative stress than control NPCs, and that oxidative stress could potentially induce some elements of senescence phenotype in these cells.

Autophagic flux is impaired in A-T NPCs

To explore other mechanisms underlying the phenotype of A-T NPCs, we studied the process of autophagy. LC3B protein is the most frequently used marker of autophagy modulation. During autophagy, LC3B-I is converted to LC3B-II through lipidation by a ubiquitin-like system involving Atg7 and Atg3, which facilitates association of LC3 with autophagic vesicles [Kabeya et al., 2000]. Western immunoblot showed that the intensity of the band of the lipidated form (LC3B-II, lower band) was higher in A-T than in control NPCs (Fig. 4A). This result may indicate either autophagy initiation or inhibition with accumulation of undigested vesicles. To distinguish between these two possibilities we looked at changes in LC3B-II after chloroquine (CQ) treatment. This compound is known to block the last stage of autophagy involving fusion of lysosomes with autophagosomes, thus affecting autophagic

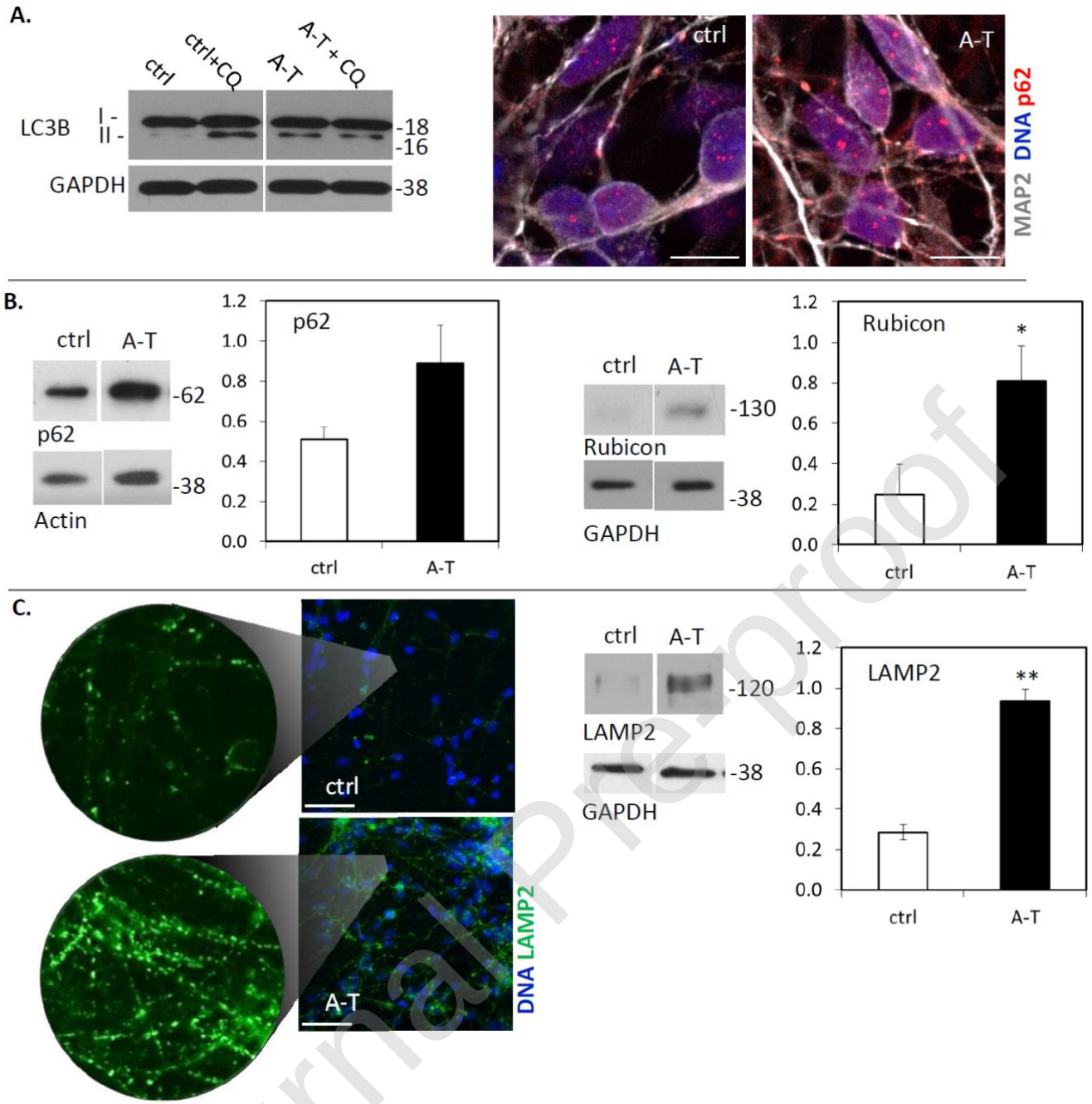

Figure 4. Autophagic flux is impaired in ATM deficient NPCs. A. Immunoblot of LC3B form I and II levels from control and A-T NPCs treated with chloroquine (n=3). Representative confocal microscopy images of p62 (red) MAP2 (grey) and DNA (blue) in control and A-T NPCs. Scale bars represent 10 µm. B. Immunoblots of p62 and Rubicon levels from control and A-T NPCs (n=3). Bars represent mean values of band intensity with SD after normalizing to GAPDH level. C. Representative images of LAMP2 (green) and DNA (blue) in control and A-T NPCs with zoomed in areas. Scale bars represent 50 µm. Immunoblot of LAMP2 level from control and A-T NPCs (n=3). Bars represent mean values of band intensity with SD after normalizing to GAPDH level.

flux [Mauthe et al., 2018]. Chloroquine treatment does not change autolysosome formation if autophagy is already blocked. In control cells we observed that CQ increased the level of LC3B-II, however this was not the case in A-T cells, in which LC3B-II, remained at same level after CQ treatment (Fig. 4A). In addition to this, we observed an increased p62 (SQSTM1) level. Protein aggregates formed by p62 are, under normal autophagic flux,

degraded by the autophagosome [Bjørkøy et al., 2006], but whenever autophagy is impaired, p62 is accumulated. Figures 4A and B provide results of staining for p62 in A-T and control NPCs and a western blot showing higher level of p62 in the former cells. The immunostaining reveals that location of p62 was not exclusively cytoplasmic, but also nuclear (Fig.4A), as reported by Hewitt et al., [Hewitt et al., 2016] in senescent fibroblasts. We also checked the presence of Rubicon protein postulated to be an internal inhibitor of autophagy [Matsunaga et al., 2009,] positively connected with the ageing process [Nakamura et al., 2019] and found its higher level in A-T NPCs in comparison to the control cells (Fig. 4B). Thus, we concluded that the elevated level of LC3B-II in A-T NPCs was a result of autophagic flux impairment.

This conclusion is in line with an elevated level of the lysosomal membrane protein - LAMP2 - in western blot analysis and an abundance of LAMP2-positive vesicles detected in immunofluorescent staining (Fig. 4C). These two results, although showing only a subpopulation of lysosomes, may point to accumulation of these vesicles.

Mitophagy may be impaired in A-T NPCs

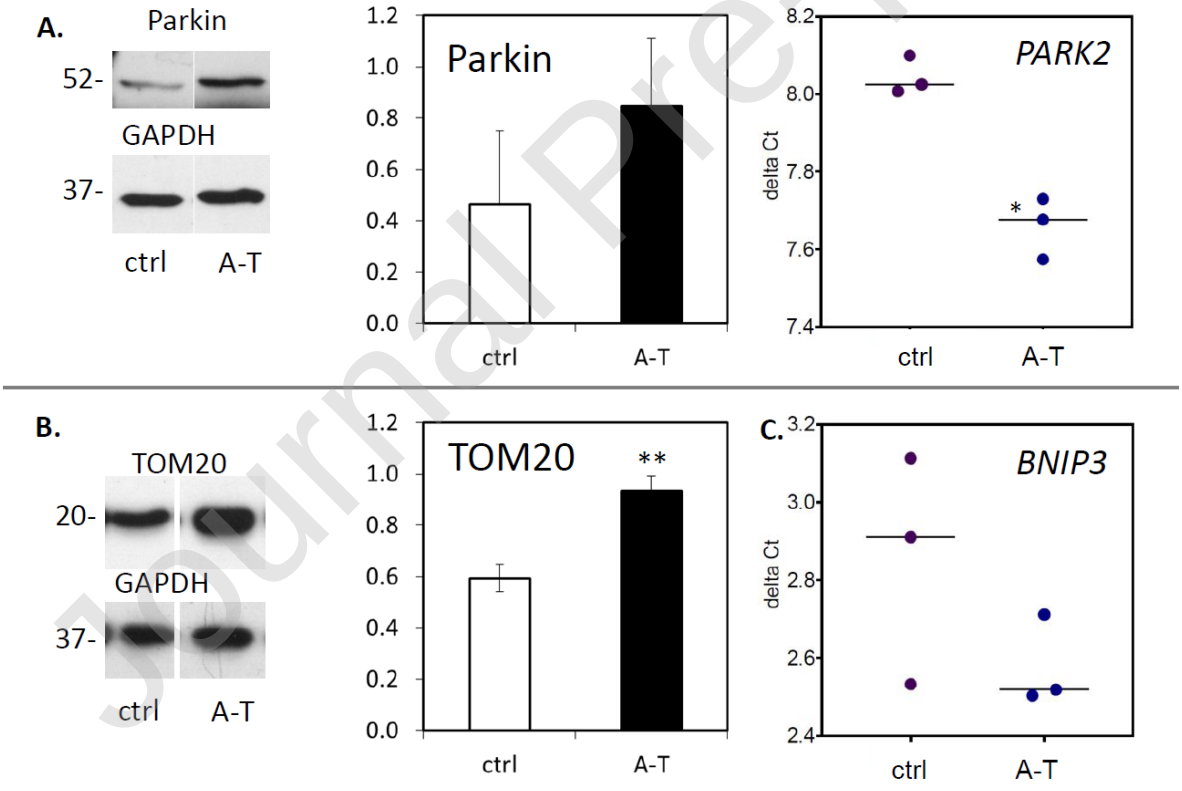

Figure 5. Mitophagy is impaired in ATM deficient NPCs. A. Immunoblot of Parkin protein from control and A-T NPCs (n=3). Bars represent mean values of band intensity with SD. Expression level of Parkin (n=3). B. Immunoblot of TOM20 protein (n=3). Bars represent mean values of band intensity with SD. C. Expression level of *BNIP3*, dots represent single experiment results, line represents median value (n=3).

Going further into consequences of impaired autophagic flux we looked closer at the process of mitophagy, that is autophagy of mitochondria. Alterations in this process have been proved to be an important factor both in cellular senescence [García-Prat et al., 2016] and in pathology of A-T [Fang et al., 2014].

Firstly, we detected a higher level of the Parkin protein in A-T NPCs in comparison with control NPCs (Fig. 5A). In dysfunctional mitochondria, the inner mitochondrial membrane becomes depolarized. This change provokes translocation of the PINK1 protein to the outer mitochondrial membrane, which, in turn, recruits Parkin (encoded by *PARK2* gene) – a cytosolic E3 ubiquitin ligase – and elicits mitophagy [Lazarou et al., 2015]. Similarly to the case of LC3B, increased level of Parkin can mean either enhanced or impaired mitophagy with accumulation of vesicles in the second case. Our further experiments pointed to the latter scenario. Mitochondrial mass, as estimated by mitochondrial outer membrane translocase TOM20 level, was significantly higher in A-T NPCs (Fig.5B). Moreover, BNIP3 – a mitophagy inducer – was expressed at a lower level in these cells as measured by RT-qPCR (Fig. 5C). BNIP3 promotes mitophagy by disrupting the Bcl-2-Beclin-1 complex and by translocating Parkin to mitochondria [Bellot et al., 2009, Lee et al., 2011]. The level of *PARK2* transcript was also downregulated, despite the protein itself being accumulated (Fig. 5A). Thus, we propose that in A-T cells, which are characterized by features of senescence, autophagy in general and mitophagy in particular, are impaired.

To further explore the relation between oxidative stress and the processes outlined above, we performed analysis of expression of selected genes related to the described phenotype of A-T NPCs. Transcriptome of NPCs untreated and treated with H_2O_2 was compared within the control and A-T group.

Interactions and functions of selected genes were analyzed using STRING - functional protein association networks (https://string-db.org/) and GeneMANIA Cytoscape plugin (https://genemania.org/). Genes selected for this experiment are markers of neurons (*MAP2*), astrocytes (*GFAP*), oxidative defense (*SOD1, OGG1*), mitophagy (*BNIP3, FUNDC1, PARK2*) and mitochondrial functionality (*MT-ATP6*). Additionally, according to STRING, five genes (*GFAP, MAP2, PARK2, SOD1, BNIP3)* are involved in cell differentiation process, of which *GFAP, PARK2* also take part in regulation of neurotransmitter uptake. Out of three genes regulating mitophagy (*BNIP3, FUNDC1, PARK2*), two (*BNIP3, PARK2*) play also an important role in negative regulation of mitochondrial fusion and positive regulation of mitochondrial fission. *MT-ATP6, OGG1, SOD1* have been implicated in ageing process and

BNIP3, *PARK2*, *OGG1*, *SOD1* in response to various forms of oxidative stress. According to GenMANIA, *ATM* gene interacts directly with *PARK2* and *BNIP3.*

Results of the expression analysis can be seen on Figure 6. Besides the differences that were already described in previous sections, like downregulation of *SOD1*, *PARK2* and *BNIP3* in A-T NPCs compared to control NPCs, some other patterns have been revealed: A-T NPCs had consequently, however not significantly, lower expression of both *MAP2* and *GFAP* markers. *OGG1* – the gene that encodes the enzyme responsible for the excision of 8-oxoguanine, a mutagenic base byproduct which occurs as a result of exposure to reactive oxygen species, was also downregulated in A-T NPCs in comparison to control NPCs. Treatment with hydrogen peroxide had clearly influenced expression of genes regulating mitophagy in the case of A-T NPCs. *PARK2* was significantly downregulated in A-T NPCs treated with hydrogen peroxide as compared to non-treated A-T NPCs (#, $p<0.05$). *FUNDC1* is an activator of mitophagy, typically induced by hypoxia induced factors, which constitutes an important mechanism for mitochondrial quality control. Similarly to *PARK2*, *FUNDC1* was downregulated after H_2O_2 treatment in A-T NPCs ($p=0.05$). We also observed a decrease in expression of mitochondrial ATP synthase membrane subunit 6 (*MT-ATP6)*, that was

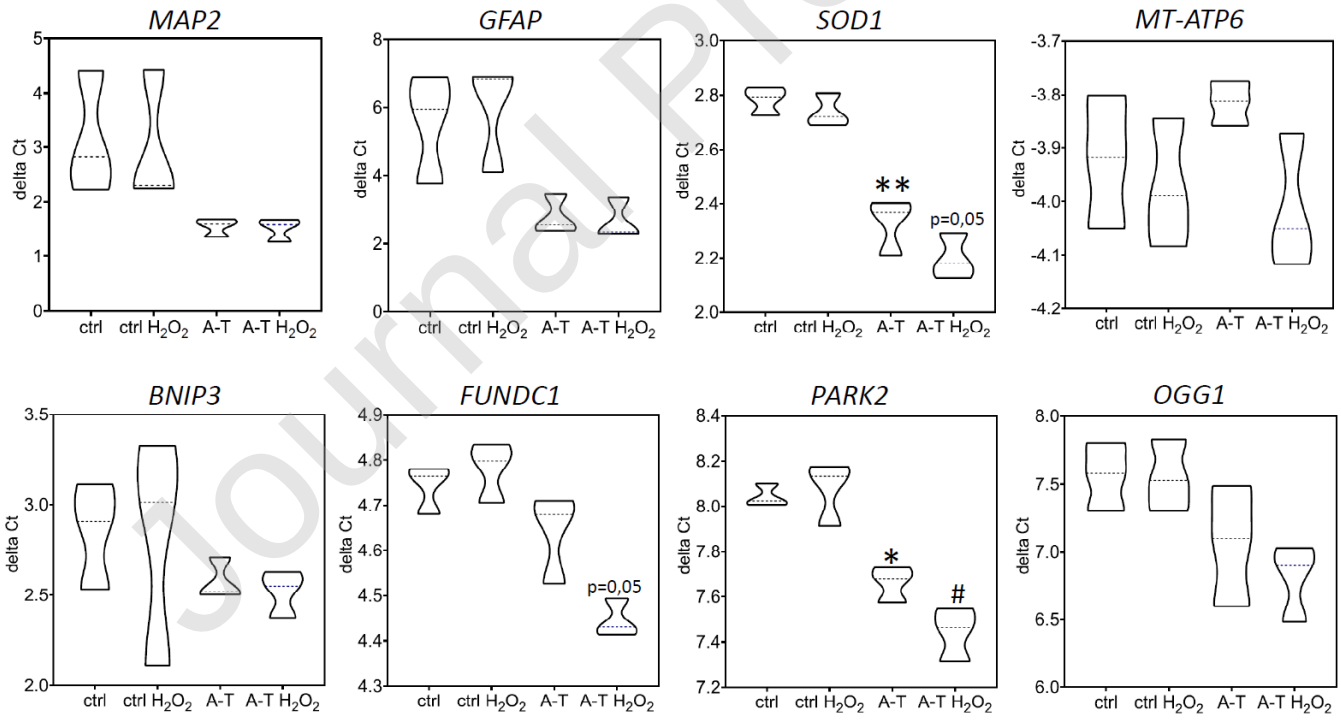

Figure 6. Real time (qRT-PCR) expression of genes in control and A-T NPCs after H_2O_2 treatment. Data presented as ΔC_t with mean. Asterisks (*) represent statistical diference to control NPCs, hashtag (#) to untreated cells (n=3).

nonsignificant, however repeating in all experiments, which may mean a drop in ATP production in A-T NPCs treated with hydrogen peroxide. Nonsignificant decrease in expression was also recorded in the case *OGG1* and *SOD1* ($p=0.05$) in A-T NPCs treated with H_2O_2 compared to untreated A-T NPCs. Treatment with hydrogen peroxide had no visible effect on control NPCs derived from healthy patient, nor on A-T NPCs in the case of *MAP2*, *GFAP* and *BNIP3*.

DISCUSSION

This study set out with the aim of elucidating the difference between NPCs derived from A-T patient and from healthy individual in terms of cell senescence and autophagy. These two processes are crucial for brain ageing, but so far have not been explored intensively at the cellular level. Having previously shown that senescence of cortical neurons in vitro is DDR-independent, we employed human neural cells lacking a key protein of this pathway (i.e. ATM) to further investigate whether this enzyme is indispensable in establishing senescence phenotype. To this end, we used hiPSCs-derived early NPCs and differentiated them to non-dividing NPCs for two weeks. Cells were cultured in oxygen conditions resembling brain physiological normoxia (5%) and showed expression of neuronal markers, namely, MAP2, β-tubulin and PSD95. Cells at this point do not express cyclin B (necessary for mitosis) as shown by Carlessi et al., [2014]

The results presented in this paper point to a number of features of A-T NPCs that are typical for senescence. Two essential markers of senescence were higher in these cells in comparison to control NPCs - SA-β-gal and SASP, together with two regulators of senescence - increased GATA4 transcription factor and decreased SIRT1. Knowing that SIRT1 inhibits NF-κB-regulated secretion of proinflammatory cytokines [Kauppinen et al., 2013], deactivates the p53 protein [Vaziri et al., 2001] and stimulates autophagy [Lee et al., 2008], this result provides another evidence of senescence in A-T NPCs. Activated p38 MAPK, one of the elements of cellular response to stress factors, is in line with a phenotype of neuronal senescence suggested by Jurk et al., [Jurk et al., 2012].

Previous studies have noted the occurrence of premature senescence in A-T cells, none of them, however, went beyond studying fibroblasts and lymphocytes. In a paper by Shiloh et al., senescence of A-T fibroblasts was assessed by a decrease in colony-forming ability at early passages [Shiloh et al., 1982]. Accelerated telomere shortening was revealed in lymphocytes [Metcalfe et al., 1996] and fibroblasts [Smilenov et al., 1997, Xia et al., 1996], while expression of the catalytic subunit of telomerase (hTERT) in these cells reversed

senescence associated traits, such as high activity of SA-β-gal, increased size and proliferation arrest [Wood et al., 2001].

These results may seem to contradict the findings of Kang et al., who showed that one of the ATM inhibitors (KU-60019) was able to alleviate DNA damage-dependent cell senescence of proliferation-competent cells [Kang et al., 2017]. However, even if chemical inhibition of ATM may have an anti-senescence effect, it does not stand contrary to the results presented above. Upon closer examination, attenuation of senescence in Kang's work is dose-dependent and may arise from the fine tuning of ATM activity, rather than from its total ablation. The authors admit that while partial ATM inhibition may induce cell proliferation, null-mutations of the *ATM* gene have no anti-senescence effects. Taking into consideration the two major roles of ATM - it is a crucial kinase in DNA damage response pathway and a sensor of reactive oxygen species (ROS), which turns on the antioxidant defense, one can speculate that a certain level of inhibition reduces only the first function, resulting in a less pronounced senescence phenotype in Kang's experiment. A complete lack of ATM, on the other hand, seems to affect also the antioxidant defense. Moreover, it cannot be excluded that ATM in non-dividing cells is more involved in the response to oxidative stress than to DNA damage. Indeed, we have shown previously that the senescence phenotype of rat cortical neurons is DDR-independent [Piechota et al., 2016].

At this point, it is important to touch upon the implications that the process of reprogramming may have on senescence and vice versa. While cellular senescence can in some cases impair successful reprogramming to pluripotent stem cells [Banito et al., 2009], even transient expression of reprogramming factors can ameliorate senescent phenotype and reverse cellular age in many types of human somatic cells at the transcriptomic, epigenetic, and cellular levels. Recently, it has been documented for the first time that chondrocytes from patients with osteoarthritis, a disease that is strongly age-related, loose their proinflammatory phenotype and epigenetic alterations after transient expression of reprogramming factors [Sarkar et al., 2020]. This does not contradict our results - even if we assume that the original A-T fibroblasts used in our experiment possessed some features of senescence that were erased in the process of reprogramming, the senescent phenotype of A-T NPCs might have developed during the differentiation period. In other words, cells may lose their senescent phenotype but do not lose the ability to acquire it again.

Our findings show oxidative stress to be associated with the observed phenotype. We showed higher levels of ROS in A-T (as compared to ATM-proficient) NPCs by 4-HNE immunoblotting. In addition to that, weaker antioxidant defense was revealed by lower levels

of *SOD1* transcript in A-T cells and by their stronger response to hyperoxia. Two weeks in 20% oxygen, but not a four-day treatment with hydrogen peroxide, resulted in higher SA-β-gal activity and IL-8 secretion. Three potential reasons for the differences observed under conditions of oxidative stress can be taken into consideration. The primary one is the dysfunction of ATM, since, as described by Guo et al [Guo et al., 2010], ATM regulates global cellular responses to oxidative stress. NADPH oxidase 4, the level of which in our model was on average 4-times higher in A-T cells, seems to be the second reason. NOX4 is an enzyme which transfers an electron from NADPH to an oxygen molecule turning it into a superoxide anion, which may successively give rise to other forms of ROS [Bedard et al., 2007]. Our finding is consistent with what has been shown by Weyemi et al. [Weyemi et al., 2015], namely, that NOX-4 level was increased both in cultured A-T fibroblasts and in post-mortem samples of various brain areas of A-T patients. It is worth noting that higher level of NOX4 was implicated in senescence of human umbilical vein endothelial cells [Lener et al., 2009] and vascular smooth muscles cells [McCrann et al., 2009]. The relation between senescence and NOX4 seems to be more complicated though, since some opposite results were reported, including our finding that NOX4 deficiency in human vascular smooth muscle cells leads to senescence with a decrease in ROS level [Przybylska et al., 2016].

Despite some changes NPCs seemed generally well protected against hydrogen peroxide, which might have been a result of generally higher antioxidant defense in NPCs as compared to terminally differentiated neurons. The level of antioxidant defense changes together with a shift towards oxidative phosphorylation during differentiation [Zheng et al., 2016], so does reaction to various agents [Augustyniak et al., 2017a, Augustyniak et al., 2017b]. Moreover, 5% oxygen concentration acts largely protective through hypoxia inducible factors [Szablowska-Gadomska et al., 2011].

Recent studies argue that the processes of autophagy and senescence are inseparable. Despite many inconsistencies in the literature, what we know so far is that maintaining autophagy can prevent senescence [García-Prat et al., 2016], autophagy impairment can induce premature senescence in human fibroblasts [Kang et al., 2011] while restoration of autophagic flux may rescue cells from senescence [Lerner et al., 2013]. This phenomenon was recently confirmed in a study on cortical neurons, where autophagy stimulation inhibited senescence [Moreno-Blas et al., 2019]. Our study revealed that senescence in A-T NPCs goes hand in hand with disturbances in autophagy. Even though the vesicular form of LCB3 was elevated, we showed accumulation of the autophagy substrate (p62), higher level of internal autophagy inhibitor (Rubicon) and no reaction to chloroquine treatment in A-T NPCs, which

points unambiguously to impaired autophagic flux. One especially interesting result was the increased number of LAMP2-positive vesicles in A-T NPCs. This observation possibly links impaired autophagy to increased SA-β-gal activity, which is in fact a lysosomal enzyme, that has been correlated with lysosomal mass by Lee et al [2006] and in our recent study on rat neurons [Piechota et al., 2016]. Both abundance of lysosomes and loss of functional autophagy can be a result of the same anomaly. In the study by Moreno-Blas et al. [2019] autophagic flux is blocked in senescent neurons *in vitro* possibly due to dysfunction of lysosomes (the same study reports unusual lysosomal morphology and immaturity) that are unable to fuse with autophagosomes. Dysfunctional lysosomes are, at the same time, a possible stimulus for further lysosomal biogenesis through nuclear translocation of TFEB transcription factor [Zhitomirsky et al., 2018]. Another result linking impaired autophagy with the senescence phenotype is the increased level of GATA4 - a transcription factor that, under normal conditions, is degraded by autophagy. Whenever this process fails, GATA4 is stabilized and activates one of the master regulators of SASP and senescence - NF-κB [Kang et al., 2015]. Looking at the changes in secretion of interleukins this seems to be the case.

Mitochondria are the site of most ROS production in the cell. Although as reported in our previous works [Grabowska et al., 2015, Przybylska et al., 2016], ROS scavenging did not alleviate cell senescence, increased mitochondrial content has been a well-documented fact in DNA damage-dependent senescence [Correia-Melo et al., 2016]. The same study presents impaired mitophagy as a feature that is strongly connected with senescence. Here we show that A-T NPCs are characterized by a possible defect in mitophagy with accumulation of Parkin protein and downregulation of of *PARK2* gene. While higher mitochondrial content (as estimated here by mitochondrial protein TOM20) does not always translate to impaired mitophagy, lower expression of *BNIP3* and less SIRT1 protein, seem to support this idea. A connection between SIRT1 and mitophagy has been established a few years ago - SIRT1 activates mitophagy by elevating NAD+/NADPH ratio [Jang et al., 2012], BNIP3 by disrupting the Bcl-2-Beclin-1 complex and by translocating Parkin to mitochondria [Bellot et al., 2009, Lee et al., 2011]. Although more evidence is needed to undoubtedly confirm our hypothesis, results from other groups prove it in other neuronal models. The work by Fang et al. [2016] shows defective mitophagy in ATM (-/-) rat primary neurons and human SH-SY5Y neuroblastoma cells. If fully confirmed in our model, dysfunctional mitochondria would be a significant source of oxidative stress in A-T NPCs.

Oxidative stress seems to be an important but not unique factor driving senescence in this model. Findings of Fang et al [Fang et al., 2016] point strongly to the NAD+/Sirtuin

signaling as a potential target for rescuing from senescence. In their research replenishment of NAD+ improved the lifespan and healthspan of ATM –/– mice and the quality of their mitochondria via restoring mitophagy. Oxidative stress has been also undoubtedly linked to mitophagy. In our results A-T NPCs treated with hydrogen peroxide displayed lower expression of *PARK2* and *FUNDC1* genes.

Overall, this paper has given an account of senescence phenotype observed in A-T NPCs. We presented these changes to be accompanied by disturbances in autophagy and mitophagy and accompanied by oxidative stress. As senescence is always defined by multiple characteristics and is especially elusive in non-dividing cells, more complete description of this phenotype would be beneficial. Future research should also investigate the occurrence of senescence *in vivo* in neurons of A-T patients and assess its impact on the symptoms of disease. If premature cell senescence is indeed identified in A-T brain, just like it has recently been in AD [Zhang et al., 2019, Musi et al., 2018] and Parkinson's disease [Chinta et al., 2018], it may possibly translate into new clinical approaches with senolytics as a new potential way of treatment.

MATERIALS AND METHODS

hiPSCs generation and neural differentiation

hiPSCs and hNPCs were obtained as described previously in Carlessi et al., 2014: A-T patient-derived primary dermal fibroblasts were purchased from the Coriell Institute for Medical Research (Camden, NJ, USA). Control fibroblasts were obtained from healthy donor matched by age and ethnicity. Fibroblasts were cultured at 37°C in a 5% CO_2 in E-MEM supplemented with 15% heat-inactivated FCS, 100 units/ml penicillin, 100 mg/ml streptomycin, 100 mM non-essential amino acids and 2mM glutamine. Fibroblasts were infected with the STEMCCA Cre-Excisable Constitutive Polycistronic Lentivirus (Millipore) following the manufacturer's instructions. After 20–25 days, hiPSC clones were picked and seeded on Matrigel (hESC-qualified matrix, BD Biosciences)-coated plates in Nutristem culture medium (Stemgent) supplemented with 100 units/ml penicillin and 100 mg/ml streptomycin.

For neural differentiation hiPSC colonies were harvested as for passaging, resuspended in hESC medium without bFGF and plated into a 6 cm low binding dish for floating cultivation. After 5 days in suspension culture, embryoid bodies (EBs) were collected and plated into a Matrigel-coated dish for additional 7 days in hESC media supplemented with 1X N2 (Gibco). After 7 days, rosettes were manually picked, mechanically dissociated

into single cells and resuspended in Neural Precursor medium (NP medium) composed of DMEM/F12 supplemented with 2mM glutamax, 100 units/ml penicillin, 100 mg/ml streptomycin, 1 : 500 B27 (Gibco), 1X N2, 20 ng/ml epidermal growth factor (EGF) and 20 ng/ml bFGF and plated into Matrigel coated flasks. NP medium was changed every 2 days. For passaging, 90% confluent cells were detached using Accutase (Life Technologies) and split at a ratio of 1 : 4. For further differentiation, proliferating hNPCs were plated in NP medium at a concentration of 5×10^3 cells/cm^2; 24 h later medium was changed to NP Medium without bFGF and EGF and replaced every 2–3 days thereafter.

The 5% oxygen concentration has been achieved by culturing cells in a multi-gas incubator with regulated CO_2 and O_2 influx. Passaging and medium changing was done in a regular hood under atmospheric conditions

NPCs H_2O_2 treatment

NPCs cultured for 14 days in NP medium without EGF and bFGF as described above were treated by 15 µM H_2O_2. Cells were harvested 4 days after the treatment.

SA-β-gal staining

The staining was performed according to the procedure published by Dimri et al., [Dimri et al., 1995]. Cell cultured on glass coverslips were washed in PBS and fixed in a solution containing 2% formaldehyde and 0,2% glutaraldehyde for 5 minutes. Following that, cells were washed twice with PBS and exposed to staining solution containing 1 mg/ml 5-bromo-4-chloro-3-indolyl-b-D-galactopyranoside, 5 mM potassium ferrocyanide, 5 mM potassium ferricyanide, 150 mM NaCl, 2 mM MgCl2, and 0.1 M phosphate buffer, pH 6.0. The staining step was done overnight in 37 °C in tightly sealed plates. Cells containing blue-dyed precipitate were considered positive and counted in bright-field microscopy. Optionally, additional staining was performed as described in the "Immunocytochemical staining" section.

Immunocytochemical staining

Cell cultured on glass coverslips were washed in PBS and fixed in 4% solution of paraformaldehyde (PFA) for 10 minutes. Fixed cells were permeabilized in 0.2% solution of Triton X 100 in PBS. The concentration of Triton was increased to 0.5% if the target protein was expected to be located in nuclei. Following this, a 10-minute blocking step was performed in 1.5% goat serum (Sigma), 2% bovine serum albumin (BSA, Sigma) and 0,1 %

Triton X 100 in PBS. Incubation with primary antibodies was held for 2 hours at room temperature with antibodies dissolved in the blocking solution. Antibodies used: rabbit anti-β-tubulin III (1:750, Covance), rabbit anti-IL6 (1:200, Abcam), rabbit anti-Ki67 (1:200, Abcam), mouse anti-LAMP2 (1:500, eBioscience), mouse anti-MAP2 (1: 200, Sigma), mouse anti-p62 (1:1000, BD Biosciences). After 3 washes in PBS cells were incubated for 1 hour with secondary antibodies, conjugated with a fluorochrome - Alexa fluor 488 anti-rabbit, Alexa fluor 488 anti-mouse, Alexa fluor 555 anti-rabbit (1:500, Life Technologies). At the end, DNA was stained by a 10 minute incubation in 2 μg/ml Hoechst solution followed by PBS and two washes with PBS.

Samples were visualized either by a fluorescent microscope or, if stated in the figure legend, by confocal laser scanning microscope. Confocal microscopy was performed using a Leica TCSP8 microscope with 63×/1.4 Leica oil immersion lens. Fluorescence was excited using the 405-nm line from a pulsed laser (for Hoechst) and a white light laser for other fluorochromes. Emitted light was captured using a hybrid Leica detector at 200 Hz scanning speed and 1024 x 1024 pixels resolution. Confocal z section stacks were collected at 0.3-μm spacing through the depth of the specimen. Final images represent a maximum projection along the z axis. All other photographs were taken by a Nikon Eclipse Ti microscope with 40x/0.6 Nikon lens. Fluorescence was excited by a metal halide lamp (Lumen 200). Pictures were captured by a DS-Fi2 or DS-Qi2 camera (Nikon).

Western blotting

Cell collection and lysis were performed using RIPA buffer (Sigma) with protease and phosphatase inhibitors. 10-15 μl of RIPA with the inhibitors was used per 1 cm^2 of a culture dish, cells were scraped and the suspension was collected on ice. After 20 minutes of incubation lysates were centrifuged at 20000 g / 4°C for 15 min. Supernatants were analyzed for protein concentration with Sigma BCA kit (Sigma) according to the manual.

Equal amounts of protein were separated electrophoretically using the Bio-Rad Mini Protean system on 8%, 10% or 12% SDS-polyacrylamide gels under 100-150 V. Proteins were then transferred to nitrocellulose membrane and blocked with 5% skimmed milk solution in TBS containing 0.1% Tween (TBST). Primary antibody incubation was carried out in a blocking solution at 4°C overnight. Antibodies used: rabbit anti-ATM (1:500, Abcam), mouse anti-GAPDH (1:50 000, Millipore), rabbit anti-GATA4 (1:500, Novus), mouse anti-LAMP2 (1:500, eBioscience), rabbit anti-LC3B (1:500, Sigma), rabbit anti-NOX4 (1:500, Abcam), mouse anti-p-p38 (1:500, Cell Signaling), rabbit anti-p38 (1:500, Cell Signaling),

mouse anti-p62 (1:1000, BD Biosciences), rabbit anti-Parkin (1:500, Abcam), mouse anti-PSD95 (1:500, Abcam), rabbit anti-Rubicon (1:250 Cell Signalling), rabbit anti-Sirt-1 (1:250, Cell Signalling), rabbit anti-TOM20 (1:1 000, Cell Signalling). After triple wash with TBST, membranes were incubated for 1 hour with HRP-conjugated secondary antibodies (anti-mouse or anti-rabbit, 1:2000, Dako) dissolved in the blocking solution. For final detection, the ECL system was used (GE Health Care) according to manufacturer's instruction. Light emission was captured as an image on an X-ray film.

Cytokine secretion measurement

Cytokine concentration was measured by the ELISA method. Medium was collected at the same time as cells and frozen at −20°C. Concentrations of the secreted proteins were measured using a colorimetric enzyme-linked immunosorbent assay according to the protocol provided by the manufacturer (R&D, Biokom, Warsaw, Poland). Standard curves were used to calculate the final results.

RNA isolation and purification

Total RNA was extracted from the analyzed cells (NP) by using Total RNA Mini (A&A Biotechnology) and purified with Clean-Up RNA Concentrator (A&A Biotechnology). The concentration of RNA was determined by using NanoDrop ND-1000 (Thermo Fisher Scientific).

qRT-PCR reaction

The RNA was converted into cDNA in the RT reaction (High-Capacity RNA-to-cDNA™ Kit, (Thermo Fisher Scientific) on was used to analyze gene expression (qRT-PCR).

The qRT-PCR reaction was performed onto Civic Cycler Thermal cycler (Biotech INC). For qRT-PCR, 10ng of cDNA were loaded with 0.25M of forward and reverse primers; 12.5µl of Sybr green (A&A Biotechnology) in the following steps: initial denaturation step at 95°C for 3min, 45 cycles of denaturation at 95°C for 10sec, and annealing/extension at 58°C for 1min. The qRT-PCR reaction was performed onto 96-well plate for LightCycler® 96 (Roche Diagnostics GmbH). The quantification cycle (Cq) values automatically calculated by the qPCR instrument software were then used for data analysis GeneEx 6.1 software (MultiD Analyses AB). Relative gene expression was determined using the ΔΔ-CT method 3. Experimentally determined PCR efficiency E(%) was in the range of 1.92-2.15. NormFinder was used for reference gene prediction.

Sequences of primers used to the reference gene validation and MAP2, GFAP genes quantification were described previously in Augustyniak et al., 2017a and Augustyniak et al., 2017b. All primers were synthesized in the MERCK company (https://www.sigmaaldrich.com/). Relative quantification in qRT-PCR was performed according to Pfafl methods. qRT-PCR results represent 3 independent experiments, each at least in 4 replicates. All primer sequences are listed in supplementary table 1.

After purification of RNA integrity index was assessed by with qRT-PCR methods based on designed along the length of the TBP (TATA-box binding protein) cDNA and calculated as a Cq difference between qRT-PCR products amplified with the 5' and 3' primers pairs., first primers pair was located close to the 3' UTR and second primer pair close to 5' end.

Statistical Analysis

At least three independent repetitions (differentiations of NPCs) were performed. For qRT-PCR results, quantification cycle (Cq) values were automatically calculated by the qPCR instrument software and used for data analysis GeneEx 6.1 software (MultiD Analyses AB). Relative gene expression was determined using the ΔΔ-CT method 3. Experimentally determined PCR efficiency E(%) was in the range of 1.92-2.15. NormFinder was used for reference gene prediction as described in Augustyniak et al., 2017a and Augustyniak et al., 2017b. Results of reference gene selection are presented in supplementary figure 2. Relative quantification in qRT-PCR was performed according to Pfafl method [Pfaffl 2001]. All results were analyzed with t-Student test or Mann Whitney test (depending on Kolmogorov–Smirnov test results) and presented as single points plot with median or as violin plot with mean. Statistical analysis was performed in Graphpad prism 5.0 software.

Acknowledgements

The study was supported by grant no. 2012/07/B/NZ3/02180 from the National Science Centre.

References

Anderson R, Lagnado A, Maggiorani D, Walaszczyk A, Dookun E, Chapman J, Birch J, Salmonowicz H, Ogrodnik M, Jurk D, Proctor C, Correia-Melo C, Victorelli S, Fielder E, Berlinguer-Palmini R, Owens A, Greaves L.C, Kolsky K.L, Parini A, Douin-Echinard V, LeBrasseur N.K, Arthur H.M, Tual-Chalot S, Schafer M.J, Roos C.M, Miller J.D, Robertson N, Mann J, Adams P.D, Tchkonia T, Kirkland J.L, Mialet-Perez J, Richardson G.D, Passos J.F. Length-independent telomere damage drives post-mitotic cardiomyocyte senescence. EMBO J. 2019;38(5):e100492.

Alexander A, Cai SL, Kim J, Nanez A, Sahin M, MacLean KH, Inoki K, Guan KL, Shen J, Person MD, Kusewitt D, Mills GB, Kastan MB, Walker CL. ATM signals to TSC2 in the cytoplasm to regulate mTORC1 in response to ROS. Proc Natl Acad Sci U S A. 2010;107(9):4153-8.

Augustyniak J, Lenart J, Zychowicz M, Lipka G, Gaj P, Kolanowska M, Stepien PP, Buzanska L. Sensitivity of hiPSC-derived neural stem cells (NSC) to Pyrroloquinoline quinone depends on their developmental stage. Toxicol In Vitro. 2017a;45(Pt 3):434-444.

Augustyniak J, Lenart J, Zychowicz M, Stepien PP, Buzanska L. Mitochondrial biogenesis and neural differentiation of human iPSC is modulated by idebenone in a developmental stage-dependent manner. Biogerontology. 2017b;18(4):665-677.

Banito A, Rashid ST, Acosta JC, Li S, Pereira CF, Geti I, Pinho S, Silva JC, Azuara V, Walsh M, Vallier L, Gil J. Senescence impairs successful reprogramming to pluripotent stem cells. Genes Dev. 2009;23(18):2134-9.

Barlow C, Dennery PA, Shigenaga MK, Smith MA, Morrow JD, Roberts LJ, Wynshaw-Boris A, Levine RL. Loss of the ataxia-telangiectasia gene product causes oxidative damage in target organs. Proc Natl Acad Sci U S A. 1999;96(17):9915-9.

Barzilai A, Schumacher B, Shiloh Y. Ataxia-telangiectasia (A-T): An emerging dimension of premature ageing. Ageing Res Rev. 2017;33:76-88.

Bedard K, Krause KH. The NOX family of ROS-generating NADPH oxidases: Physiology and pathophysiology. Physiol Rev. 2007;87(1):245–313.

Bellot G, Garcia-Medina R, Gounon P, Chiche J, Roux D, Pouysségur J, Mazure NM. Hypoxia-induced autophagy is mediated through hypoxia-inducible factor induction of BNIP3 and BNIP3L via their BH3 domains. Mol Cell Biol. 2009;29(10):2570-81.

Bjørkøy G, Lamark T, Brech A, Outzen H, Perander M, Overvatn A, Stenmark H, Johansen T. P62/SQSTM1: a missing link between protein aggregates and the autophagy machinery. Autophagy. 2006;2(2):138-9.

Campisi, J. Cellular senescence: putting the paradoxes in perspective. Curr.Opin. Genet. Dev. 2011;21:107–112.

Carlessi L, Fusar Poli E, Bechi G, Mantegazza M, Pascucci B, Narciso L, Dogliotti E, Sala C, Verpelli C, Lecis D, Delia D. Functional and molecular defects of hiPSC-derived neurons from patients with ATM deficiency. Cell Death Dis. 2014;5:e1342.

Chinta SJ, Woods G, Demaria M, Rane A, Zou Y, McQuade A, Rajagopalan S, Limbad C, Madden DT, Campisi J, Andersen JK. Cellular Senescence Is Induced by the Environmental Neurotoxin Paraquat and Contributes to Neuropathology Linked to Parkinson's Disease.Cell Rep. 2018;22(4):930-940.

Choy KR, Watters DJ. Neurodegeneration in ataxia-telangiectasia: Multiple roles of ATM kinase in cellular homeostasis. Dev Dyn. 2018;247(1):33-46.

Correia-Melo C, Marques FD, Anderson R, Hewitt G, Hewitt R, Cole J, Carroll BM, Miwa S, Birch J, Merz A, Rushton MD, Charles M, Jurk D, Tait SW, Czapiewski R, Greaves L, Nelson G, Bohlooly-Y M, Rodriguez-Cuenca S, Vidal-Puig A, Mann D, Saretzki G, Quarato G, Green DR, Adams PD, von Zglinicki T, Korolchuk VI, Passos JF. Mitochondria are required for pro-ageing features of the senescent phenotype. EMBO J. 2016; 35(7):724-42.

Cosentino C, Grieco D, Costanzo V. ATM activates the pentose phosphate pathway promoting anti-oxidant defence and DNA repair. EMBO J. 2011;30(3):546-55.

Dimri GP, Lee X, Basile G, Acosta M, Scott G, Roskelley C, Medrano EE, Linskens M, Rubelj I, Pereira-Smith O. A biomarker that identifies senescent human cells in culture and in aging skin in vivo. Proc Natl Acad Sci U S A. 1995;92:9363-9367

Fang EF, Scheibye-Knudsen M, Brace LE, Kassahun H, SenGupta T, Nilsen H, Mitchell JR, Croteau DL, Bohr VA. Defective mitophagy in XPA via PARP-1 hyperactivation and NAD(+)/SIRT1 reduction. Cell. 2014;157(4):882-896

Fang EF, Kassahun H, Croteau DL, Scheibye-Knudsen M, Marosi K, Lu H, Shamanna RA, Kalyanasundaram S, Bollineni RC, Wilson MA, Iser WB, Wollman BN, Morevati M, Li J7, Kerr JS, Lu Q, Waltz TB, Tian J, Sinclair DA8, Mattson MP9, Nilsen H, Bohr VA10. NAD+ Replenishment Improves Lifespan and Healthspan in Ataxia Telangiectasia Models via Mitophagy and DNA Repair. Cell Metab. 2016;24(4):566-581.

Freund A, Patil C.K, Campisi J. p38MAPK is a novel DNA damage response-independent regulator of the senescence-associated secretory phenotype. EMBO J. 2011;30: 1536-1548.

Fridovich I. Superoxide dismutases. An adaptation to a paramagnetic gas. J Biol Chem. 1989;264(14):7761-4.

García-Prat L, Martínez-Vicente M, Perdiguero E, Ortet L, Rodríguez-Ubreva J, Rebollo E, Ruiz-Bonilla V, Gutarra S, Ballestar E, Serrano AL, Sandri M, Muñoz-Cánoves P. Autophagy maintains stemness by preventing senescence. Nature. 2016;529(7584):37-42.

Geng Y.Q, Guan J.T, Xu X.H, Fu Y.C. Senescence-associated beta-galactosidase activity expression in aging hippocampal neurons. Biochem Biophys Res Commun. 2010;396:866-869.

Gewirtz D.A. Autophagy and senescence: a partnership in search of definition. Autophagy. 2013;9:808-812.

Grabowska W, Kucharewicz K, Wnuk M, Lewinska A, Suszek M, Przybylska D, Mosieniak G, Sikora E, Bielak-Zmijewska A. Curcumin induces senescence of primary human cells building the vasculature in a DNA damage and ATM-independent manner. Age (Dordr). 2015 ;37(1):9744

Grabowska W, Sikora E, Bielak-Zmijewska A. Sirtuins, a promising target in slowing down the ageing process. Biogerontology. 2017;18(4):447-476.

Guo Z, Kozlov S, Lavin MF, Person MD, Paull TT. ATM activation by oxidative stress. Science. 2010;330(6003):517-21.

Hewitt G, Carroll B, Sarallah R, Correia-Melo C, Ogrodnik M, Nelson G, Otten EG, Manni D, Antrobus R, Morgan BA, von Zglinicki T, Jurk D, Seluanov A, Gorbunova V, Johansen T, Passos JF, Korolchuk VI. SQSTM1/p62 mediates crosstalk between autophagy and the UPS in DNA repair. Autophagy. 2016;12(10):1917-1930.

Jang SY, Kang HT, Hwang ES. Nicotinamide-induced mitophagy: event mediated by high NAD+/NADH ratio and SIRT1 protein activation. J Biol Chem. 2012;287(23):19304-14.

Jurk D, Wang C, Miwa S, Maddick M, Korolchuk V, Tsolou A, Gonos ES, Thrasivoulou C, Saffrey MJ, Cameron K, von Zglinicki T. Postmitotic neurons develop a p21-dependent senescence-like phenotype driven by a DNA damage response. Aging Cell.2012;11:996-1004.

Kabeya Y, Mizushima N, Ueno T, Yamamoto A, Kirisako T, Noda T, Kominami E, Ohsumi Y, Yoshimori T. LC3, a mammalian homologue of yeast Apg8p, is localized in autophagosome membranes after processing. EMBO J. 2000;19(21):5720-8

Kamsler A, Daily D, Hochman A, Stern N, Shiloh Y, Rotman G, Barzilai A. Increased oxidative stress in ataxia telangiectasia evidenced by alterations in redox state of brains from Atm-deficient mice. Cancer Res. 2001;61(5):1849-54.

Kang C, Xu Q, Martin TD, Li MZ, Demaria M, Aron L, Lu T, Yankner BA, Campisi J, Elledge SJ. The DNA damage response induces inflammation and senescence by inhibiting autophagy of GATA4. Science. 2015;349(6255)

Kang C, Elledge SJ. How autophagy both activates and inhibits cellular senescence.Autophagy. 2016;12(5):898-9.

Kang HT, Lee KB, Kim SY, Choi HR, Park SC. Autophagy impairment induces premature senescence in primary human fibroblasts. PLoS One. 2011;6(8):e23367.

Kang HT, Park JT, Choi K, Kim Y, Choi HJC, Jung CW, Lee YS, Park SC. Chemical screening identifies ATM as a target for alleviating senescence. Nat Chem Biol. 2017;13(6):616-623.

Kauppinen A, Suuronen T, Ojala J, Kaarniranta K, Salminen A. Antagonistic crosstalk between NF-κB and SIRT1 in the regulation of inflammation and metabolic disorders. Cell Signal. 2013;25(10):1939-48.

Kirkland J.L, Tchkonia T. Cellular Senescence: A Translational Perspective. EBioMedicine. 2017;21:21-28.

Kuilman T, Michaloglou C, Mooi W.J, Peeper D.S. The essence of senescence. Genes Dev. 2010;24:2463-2479.

Lazarou M1. Keeping the immune system in check: a role for mitophagy. Immunol Cell Biol. 2015;93(1):3-10.

Lee BY, Han JA, Im JS, Morrone A, Johung K, Goodwin EC, Kleijer WJ, DiMaio D, Hwang ES. Senescence-associated beta-galactosidase is lysosomal beta-galactosidase. Aging Cell. 2006;5:187-195

Lee IH, Cao L, Mostoslavsky R, Lombard DB, Liu J, Bruns NE, Tsokos M, Alt FW, Finkel T. A role for the NAD-dependent deacetylase Sirt1 in the regulation of autophagy. Proc Natl Acad Sci U S A. 2008;105(9):3374-9.

Lee Y, Lee HY, Hanna RA, Gustafsson ÅB. Mitochondrial autophagy by Bnip3 involves Drp1-mediated mitochondrial fission and recruitment of Parkin in cardiac myocytes. Am J Physiol Heart Circ Physiol. 2011;301(5):H1924-31

Lee SA, Dritschilo A, Jung M. Role of ATM in oxidative stress-mediated c-Jun phosphorylation in response to ionizing radiation and CdCl2. J Biol Chem. 2001;276(15):11783-90.

Lener B, Kozieł R, Pircher H, Hütter E, Greussing R, Herndler-Brandstetter D, Hermann M, Unterluggauer H, Jansen-Dürr P. The NADPH oxidase NOX4 restricts the replicative lifespan of human endothelial cells. Biochem J. 2009;423(3):363-74.

Lerner C, Bitto A, Pulliam D, Nacarelli T, Konigsberg M, Van Remmen H, Torres C, Sell C. Reduced mammalian target of rapamycin activity facilitates mitochondrial retrograde signaling and increases life span in normal human fibroblasts. Aging Cell. 2013;12(6):966-77.

Li J, Han YR, Plummer MR, Herrup K. Cytoplasmic ATM in neurons modulates synaptic function. Curr Biol. 2009;19(24):2091-6.

Lipinski MM, Zheng B, Lu T, Yan Z, Py BF, Ng A, Xavier RJ, Li C, Yankner BA, Scherzer CR, Yuan J. Genome-wide analysis reveals mechanisms modulating autophagy in normal brain aging and in Alzheimer's disease. Proc Natl Acad Sci U S A. 2010;107(32):14164-9.

López-Otin C, Blasco MA, Partridge L, Serrano M, Kroemer G. The hallmarks of aging. Cell. 2013;153:1194–1217.

Matsunaga K, Saitoh T, Tabata K, Omori H, Satoh T, Kurotori N, Maejima I, Shirahama-Noda K, Ichimura T, Isobe T, Akira S, Noda T, Yoshimori T. Two Beclin 1-binding proteins, Atg14L and Rubicon, reciprocally regulate autophagy at different stages. Nat Cell Biol. 2009;11(4):385-96.

Mauthe M, Orhon I, Rocchi C, Zhou X, Luhr M, Hijlkema K.J, Coppes R.P, Engedal N, Mari M, Reggiori F. Chloroquine inhibits autophagic flux by decreasing autophagosome-lysosome fusion. Autophagy. 2018;4:1435-1455.

McCrann DJ, Yang D, Chen H, Carroll S, Ravid K. Upregulation of NOX4 in the aging vasculature and its association with smooth muscle cell polyploidy. Cell Cycle. 2009;8:902-908.

Metcalfe JA, Parkhill J, Campbell L, Stacey M, Biggs P, Byrd PJ, Taylor AM. Accelerated telomere shortening in ataxia telangiectasia. Nat. Genet. 1996;13:350–353.

Moreno-Blas D, Gorostieta-Salas E, Pommer-Alba A, Muciño-Hernández G, Gerónimo-Olvera C, Maciel-Barón LA, Konigsberg M, Massieu L, Castro-Obregón S. Cortical neurons develop a senescence-like phenotype promoted by dysfunctional autophagy. Aging (Albany NY). 2019;11(16):6175-6198

Musi N, Valentine J.M, Sickora K.R, Baeuerle E, Thompson C.S, Shen Q, Orr ME. Tau protein aggregation is associated with cellular senescence in the brain. Aging Cell. 2018;17:e12840.

Nakamura S, Oba M, Suzuki M, Takahashi A, Yamamuro T, Fujiwara M, Ikenaka K,Minami S, Tabata N, Yamamoto K, Kubo S, Tokumura A, Akamatsu K, Miyazaki Y,Kawabata T, Hamasaki M, Fukui K, Sango K, Watanabe Y, Takabatake Y, Kitajima TS, Okada Y, Mochizuki H, Isaka Y, Antebi A, Yoshimori T. Suppression of autophagic activity by Rubicon is a signature of aging. Nat Commun. 2019;10(1):847.

Pfaffl MW. A new mathematical model for relative quantification in real-time RT-PCR. Nucleic Acids Res. 2001 May 1;29(9):e45.

Piechota M, Sunderland P, Wysocka A, Nalberczak M, Sliwinska MA, Radwanska K, Sikora E. Is senescence-associated β-galactosidase a marker of neuronal senescence? Oncotarget. 2016;7(49):81099-81109.

Polubotko EA, Smirnova NV, Pleskach NM, Mikhelson VM, Spivak IM. Premature aging syndrome in ataxia telangiectasia patients. Cell and Tissue Biology. 2009;3:491.

Przybylska D, Janiszewska D, Goździk A, Bielak-Zmijewska A, Sunderland P, Sikora E, Mosieniak G. NOX4 downregulation leads to senescence of human vascular smooth muscle cells. Oncotarget. 2016 Oct 11;7(41):66429-66443

Rodier F, Coppé JP, Patil CK, Hoeijmakers WA, Muñoz DP, Raza SR, Freund A, Campeau E, Davalos AR, Campisi J. Persistent DNA damage signalling triggers senescence-associated inflammatory cytokine secretion. Nat Cell Biol. 2009;11:973-979.

Sapieha P, Mallette FA. Cellular Senescence in Postmitotic Cells: Beyond Growth Arrest. Trends Cell Biol. 2018;28(8):595-607.

Sarkar TJ, Quarta M, Mukherjee S, Colville A, Paine P, Doan L, Tran CM, Chu CR, Horvath S, Qi LS, Bhutani N, Rando TA, Sebastiano V. Transient non-integrative expression of nuclear reprogramming factors promotes multifaceted amelioration of aging in human cells. Nat Commun. 2020;11(1):1545.

Shiloh Y, Tabor E, Becker Y. Colony-forming ability of ataxia-telangiectasia skin fibroblasts is an indicator of their early senescence and increased demand for growth factors. Exp Cell Res. 1982;140(1):191-9.

Shiloh Y, Ziv Y. The ATM protein kinase: regulating the cellular response to genotoxic stress, and more. Nat Rev Mol Cell Biol. 2013;14(4):197-210.

Sikora E, Bielak-Zmijewska A, Mosieniak G. Targeting normal and cancer senescent cells as a strategy of senotherapy. Ageing Res Rev. 2019;55:100941

Smilenov LB, Morgan SE, Mellado W, Sawant SG, Kastan MB, Pandita TK. Influence of ATM function on telomere metabolism. Oncogene.1997;15:2659–2665.

Stagni V, Cirotti C, Barilà D. Ataxia-Telangiectasia Mutated Kinase in the Control of Oxidative Stress, Mitochondria, and Autophagy in Cancer: A Maestro With a Large Orchestra. Front Oncol. 2018;8:73.

Szablowska-Gadomska I, Zayat V, Buzanska L. Influence of low oxygen tensions on expression of pluripotency genes in stem cells. Acta Neurobiol Exp (Wars). 2011;71(1):86-93.

van Deursen JM. The role of senescent cells in ageing. Nature. 2014;509:439–446.

Vaziri H, Dessain SK, Ng Eaton E, Imai SI, Frye RA, Pandita TK, Guarente L, Weinberg RA. hSIR2(SIRT1) functions as an NAD-dependent p53 deacetylase. Cell. 2001;107(2):149-59.

Ward AJ, Olive PL, Burr AH, Rosin MP. Response of fibroblast cultures from ataxia-telangiectasia patients to reactive oxygen species generated during inflammatory reactions. Environ Mol Mutagen. 1994;24(2):103-11.

Weyemi U, Redon CE, Aziz T, Choudhuri R, Maeda D, Parekh PR, Bonner MY, Arbiser JL, Bonner WM. NADPH oxidase 4 is a critical mediator in Ataxia telangiectasia disease. Proc Natl Acad Sci U S A. 2015;112(7):2121-6.

Wood LD, Halvorsen TL, Dhar S, Baur JA, Pandita RK, Wright WE, Hande MP, Calaf G, Hei TK, Levine F, Shay JW, Wang JJ, Pandita TK. Characterization of ataxia telangiectasia fibroblasts with extended life-span through telomerase expression. Oncogene. 2001;20(3):278-88.

Xia, S.J., Shammas, M.A., Shmookler Reis, R.J., 1996. Reduced telomere length in ataxia-telangiectasia fibroblasts. Mutat. Res. 364, 1–11.

Yang Y, Herrup K. Loss of neuronal cell cycle control in ataxia-telangiectasia: a unified disease mechanism. J Neurosci. 2005;25(10):2522-9.

Zhang P, Kishimoto Y, Grammatikakis I, Gottimukkala K, Cutler RG, Zhang S, Abdelmohsen K, Bohr VA, Misra Sen J, Gorospe M, Mattson MP. Senolytic therapy alleviates Aβ-associated oligodendrocyte progenitor cell senescence and cognitive deficits in an Alzheimer's disease model. Nat Neurosci. 2019;22(5):719-728.

Zheng X, Boyer L, Jin M, Mertens J, Kim Y, Ma L, Ma L, Hamm M, Gage FH, Hunter T. Metabolic reprogramming during neuronal differentiation from aerobic glycolysis to neuronal oxidative phosphorylation. Elife.2016;5:e13374.

Zhitomirsky B, Yunaev A, Kreiserman R, Kaplan A, Stark M, Assaraf YG. Lysosomotropic drugs activate TFEB via lysosomal membrane fluidization and consequent inhibition of mTORC1 activity. Cell Death Dis. 2018;9(12):1191.

Figure 1. Characterization of hiPSCs-derived NPCs. A. Representative brightfield images of NPCs differentiated for 14 days. All of the subsequent images represent NPCs after 14 days of differentiation. Scale bars represent 50 µm. B. Representative images of Ki67 (green) and MAP2 (red) staining in A-T and control NPCs. Positive nuclei indicated by arrows. Scale bars represent 50 µm. C. Representative images of β-tubulin type III (green) immunostaining in A-T and control NPCs. Scale bars represent 50 µm. D. Representative immunoblots showing the level of PSD95 and ATM proteins in A-T and control NPCs (n=3).

Figure 2. ATM-deficient NPCs exhibit senescence-like features. A. Representative images of SA-β-gal (blue) staining in control and A-T NPCs after 14-day differentiation (bottom images). Cells have been additionally stained for MAP2 in green and DNA in blue (top images). Top and bottom pictures represent the same areas. Scale bars represent 50 µm. Quantification of SA-β-gal staining. NPCs positive for both MAP2 and SA-β-gal were counted and divided by the total number of cells, as estimated by the number of nuclei (n=3). B. Senescence associated inflammatory cytokines. Representative confocal microscopy images of Interleukin 6 (magenta) and MAP2 (green) showing production of IL-6 in A-T NPCs. Scale bar represents 25 µm. ELISA test for IL-6 and IL-8 showing the level of secretion to medium (n=5). C. Immunoblots of SIRT1, GATA4 and p-p38 protein levels from control and A-T NPCs (n=3). Bars represent mean values of band intensity with SD after normalizing to GAPDH level.

Figure 3. Senescent-like phenotype in ATM-deficient NPCs is partially oxidative-stress dependent. A. Immunoblot of NOX4 protein from control and A-T neural NPCs (n=3). Bars represent mean values of band intensity with SD. B. Immunoblot of 4-HNE protein modification (n=3). Expression level of *SOD1* (n=3). *C*. Quantification of SA-β-gal staining and IL-6 and IL-8 secretion in cells treated with hydrogen peroxide (n=3).
D. Quantification of SA-β-gal staining (n=2) and IL-8 secretion under normoxic (5% oxygen) and hyperoxic (20% oxygen) conditions (n=3).

Figure 4. Autophagic flux is impaired in ATM deficient NPCs. A. Immunoblot of LC3B form I and II levels from control and A-T NPCs treated with chloroquine (n=3). Representative confocal microscopy images of p62 (red) MAP2 (grey) and DNA (blue) in control and A-T NPCs. Scale bars represent 10 µm. B. Immunoblots of p62 and Rubicon levels from control and A-T NPCs (n=3). Bars represent mean values of band intensity with SD after normalizing to GAPDH level. C. Representative images of LAMP2 (green) and DNA (blue) in control and A-T NPCs with zoomed in areas. Scale bars represent 50 µm. Immunoblot of LAMP2 level from control and A-T NPCs (n=3). Bars represent mean values of band intensity with SD after normalizing to GAPDH level.

Figure 5. Mitophagy is impaired in ATM deficient NPCs. A. Immunoblot of Parkin protein from control and A-T NPCs (n=3). Bars represent mean values of band intensity with SD. Expression level of Parkin (n=3). B. Immunoblot of TOM20 protein (n=3). Bars represent mean values of band intensity with SD. C. Expression level of *BNIP3*, dots represent single experiment results, line represents median value (n=3).

Figure 6. Real time (qRT-PCR) expression of genes in control and A-T NPCs after H2O2 treatment. Data presented as ΔCt with mean. Asterisks (*) represent statistical diference to control NPCs, hashtag (#) to untreated cells (n=3).

Supplementary table 1. Primers used in qRT-PCR including reference genes. F – forward, R – reverse.

Supplementary Figure 1. Validation of housekeeping genes in control and A-T NPCs after H2O2 treatment using NormFinder algorithm. A. The stability of gene expression: the lowest values correspond to the most stable genes. B. Determination of the optimal number of reference genes for

normalization of control and A-T NPCs after H2O2 treatment based on the calculation of the Acc. S.D. As a result of normalization procedure the NormFinder algorithm suggested to use ACTB as a reference gene.

Supplementary Figure 2. Cytoscape network showing *in silico* prediction of gene interactions (FDR<0.001) between *BNIP3, FUNDC1, GFAP, MAP2, MT-ATP6, OGG1, PARK2, SOD1* and *ATM*